Supplementary figures legend

Suppl Figure 1. Body weight (A), lean mass (B), fat mass (C) at baseline (black bars) and at the end of the study (white bars) in the saline, exenatide and SHAM groups. Panel D: Food intake during the study in the three study groups.
Number of baboons: 12 in exenatide group, 12 in saline group and 4 in SHAM group. Comparisons between baseline and after treatment data were performed by Wilcoxon test.

Suppl Figure 2. A) Dynamics of plasma glucose concentration during the 2-step hyperglycemic clamps performed before (●) and after (□) treatments with exenatide (upper panels), saline (middle panels) and saline in SHAM-operated (bottom panels).
B) Dynamics of plasma glucagon concentration during the 2-stephyperglycemic clamps performed before (●) and after (□) treatments with exenatide (upper panels), saline (middle panels) and saline in SHAM-operated (bottom panels).
Number of baboons: 12 in exenatide group, 12 in saline group and 4 in SHAM group. Comparisons between baseline and after treatment data were performed by Wilcoxon test.

Suppl Figure 3. A) Insulin sensitivity assessed as M value in exenatide, saline and SHAM groups at baseline (black bars) and at study end (white bars). B) Relationship between insulin sensitivity and secretion at baseline and study end in exenatide, saline and SHAM groups. C) Hepatic insulin clearance in exenatide, saline and SHAM groups at baseline (black bars) and at study end (white bars). Number of baboons: 12 in exenatide group, 12 in saline group and 4 in SHAM group. Comparisons between baseline and after treatment data were performed by Wilcoxon test.

Suppl Figure 4. Insulin signaling in the skeletal muscle after treatment with exenatide (white bars) and saline (black bars). Treatment with exenatide induced a significant increase in the levels of p-Akt ser473.
Number of baboons: 12 exenatide-treated baboons vs 12 saline-treated baboons. Comparison between the two groups was performed by Mann-Whitney test.

Suppl Figure 5. Insulin signaling in the liver after treatment with exenatide (white bars) and saline (black bars). Liver of exenatide-treated baboons showed only a significant decrease of ERK

phosphorylation.
Number of baboons: 12 exenatide-treated baboons vs 12 saline-treated baboons. Comparison between the two groups was performed by Mann-Whitney test.

Suppl Figure 6. Staining for Ki67 (panel A), M30 (panel B), and c-Kit (panel C) before and after treatment in the saline and exenatide groups.

Suppl Figure 7. Representative photographs of immunofluorescence performed on pancreatic sections double stained with insulin (red) and the replication marker Ki67 (green) before (basal) and after treatment with saline (upper panels) and exenatide (lower panels). Ki67-positive nuclei (arrows) were found only in the islets of exenatide-treated baboons. The outline of the islets is shown in white.

Suppl Figure 8. Representative photographs of immunofluorescence performed on pancreatic sections double stained with glucagon (red) and the replication marker Ki67 (green) before (basal) and after treatment with saline (upper panel) and exenatide (lower panel). Ki67-positive nuclei (arrows) were found only in the islets of exenatide-treated baboons. The outline of the islets is shown in white.

Suppl Figure 9. Representative photographs of immunofluorescence performed on pancreatic sections double stained with insulin (red) and c-Kit (green) before (basal) and after treatment with saline (upper panels) and exenatide (lower panels). C-Kit-positive cells (arrows) were found only in the islets of exenatide-treated baboons. The outline of the islets is shown in white. * no specific staining.

Suppl Figure 10. Representative photographs of immunofluorescence performed on pancreatic sections double stained with insulin (red) and somatostatin (green) before (basal) and after treatment with saline (upper panels) and exenatide (lower panels). The outline of the islets is shown in white.

Suppl Figure 11. Electron microscopy of pancreatic specimens taken before (panels A, C, E and G) and after treatment with saline (panels B,D) or exenatide (F,H). Before treatments, both β- and α-cells appear healthy and well granulated. After treatment with saline (B, D) both cell types showed degenerative features including pycnotic nuclei and dark cytoplasm indicative of ongoing

apoptosis and poorly granulated β-cells (D). Conversely, after exenatide treatment (F, H) β- and α-cells continued to appear healthy and well granulated.

Suppl Figure 12. Dynamics of plasma proinsulin concentrations during the 2-step hyperglycemic clamps performed before (●) and after (□) treatments with exenatide (A) and saline (B).

Suppl. Figure 1

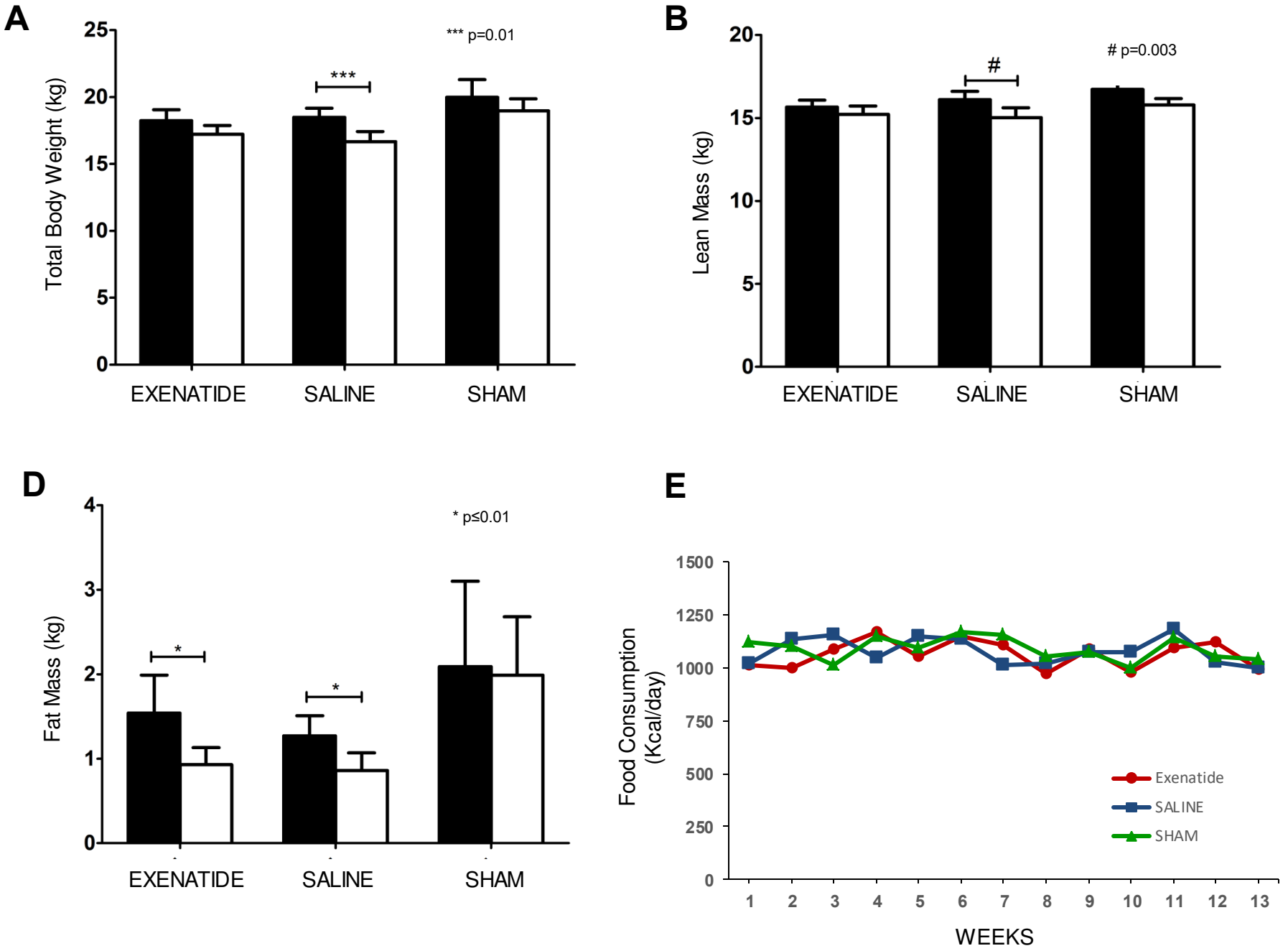

Suppl. Figure 2

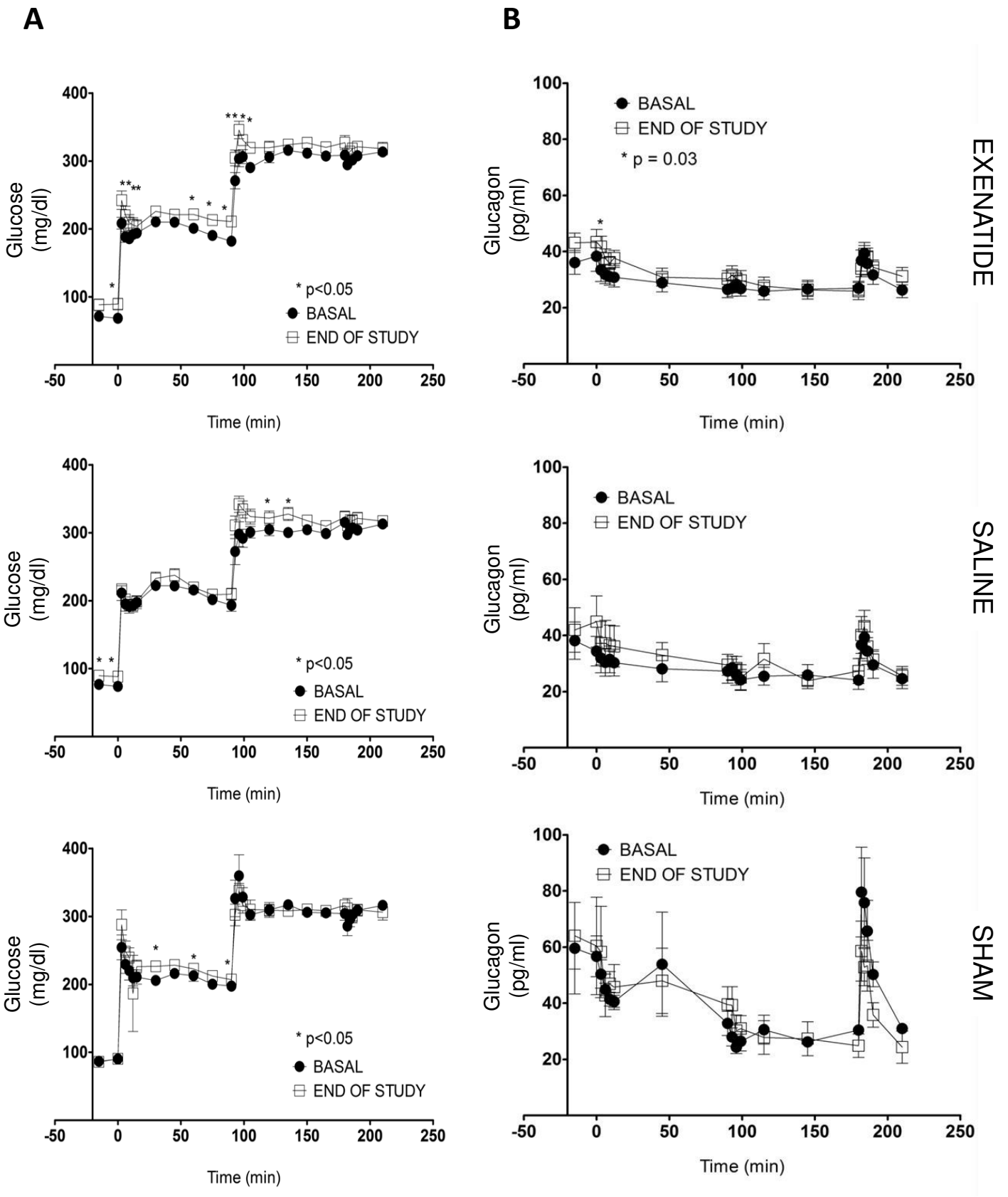

Suppl. Figure 3

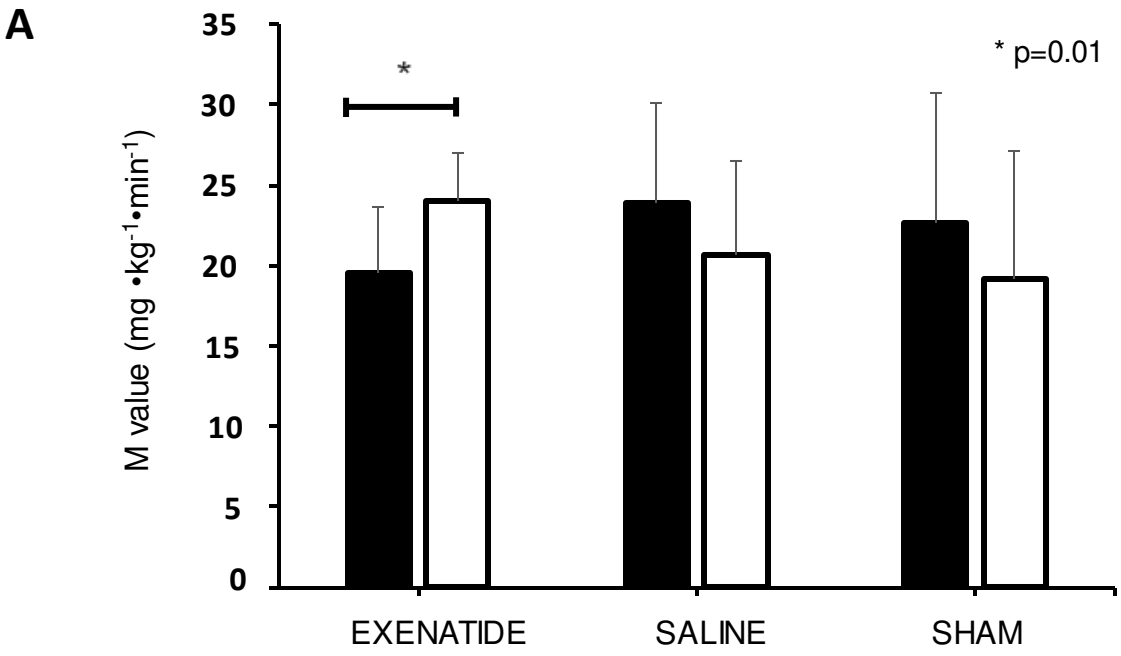

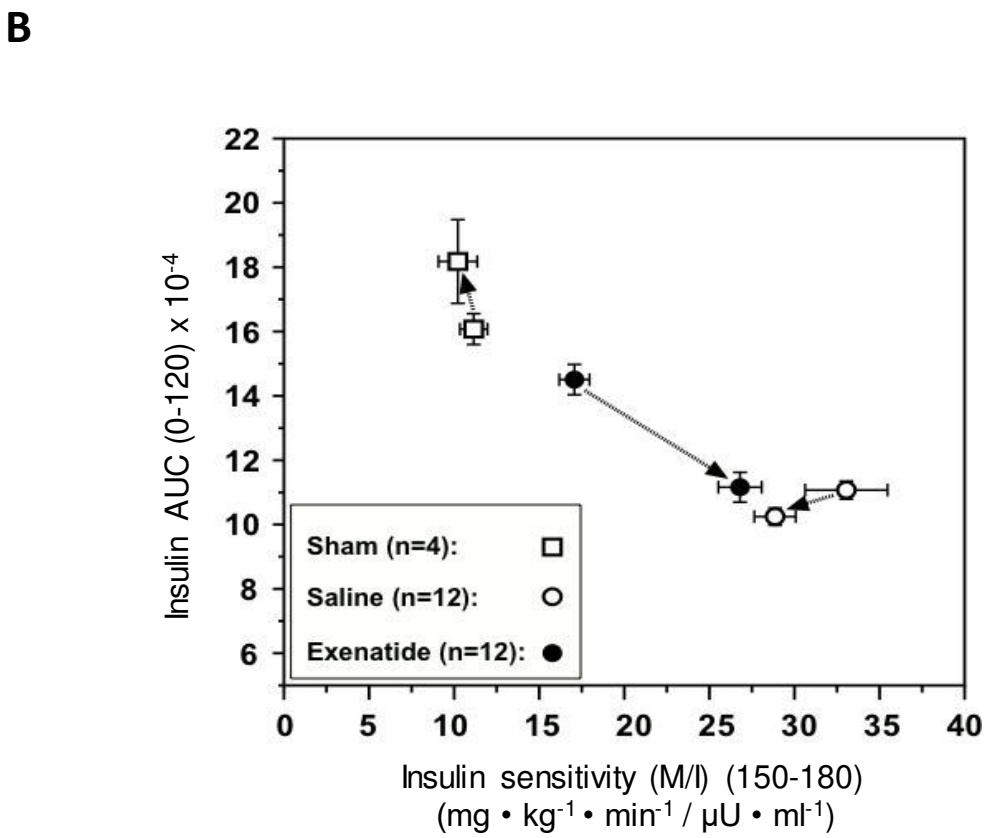

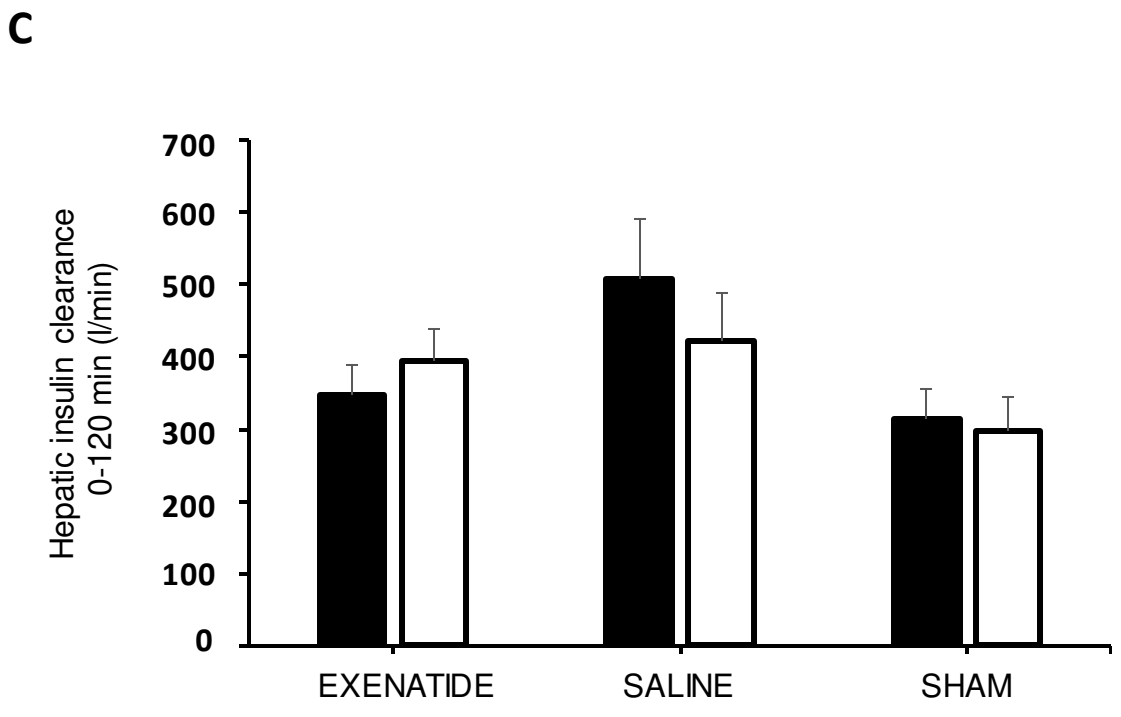

Suppl. Figure 4

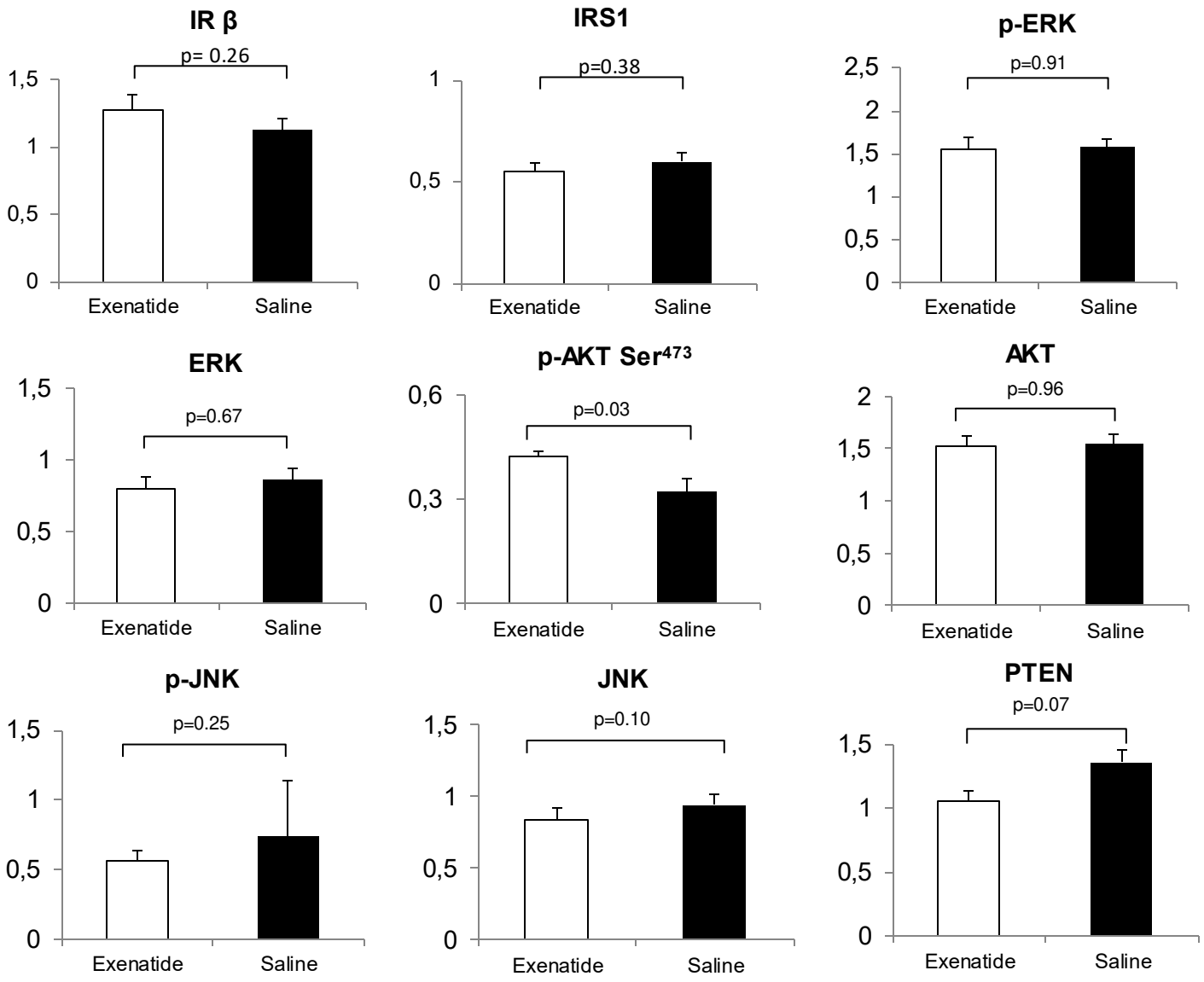

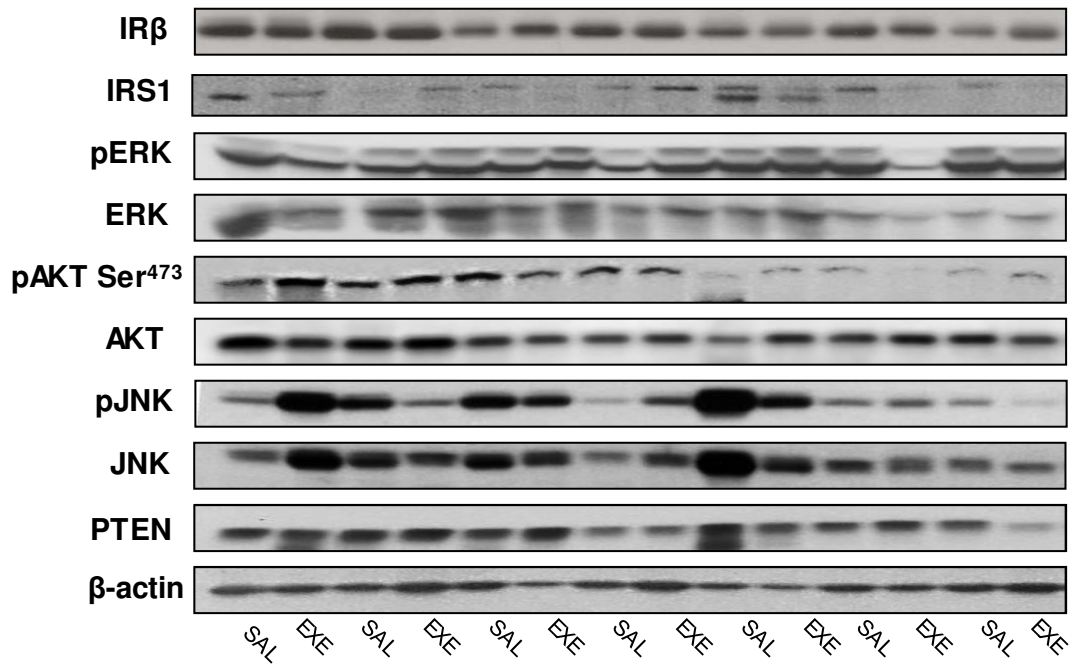

Suppl. Figure 5

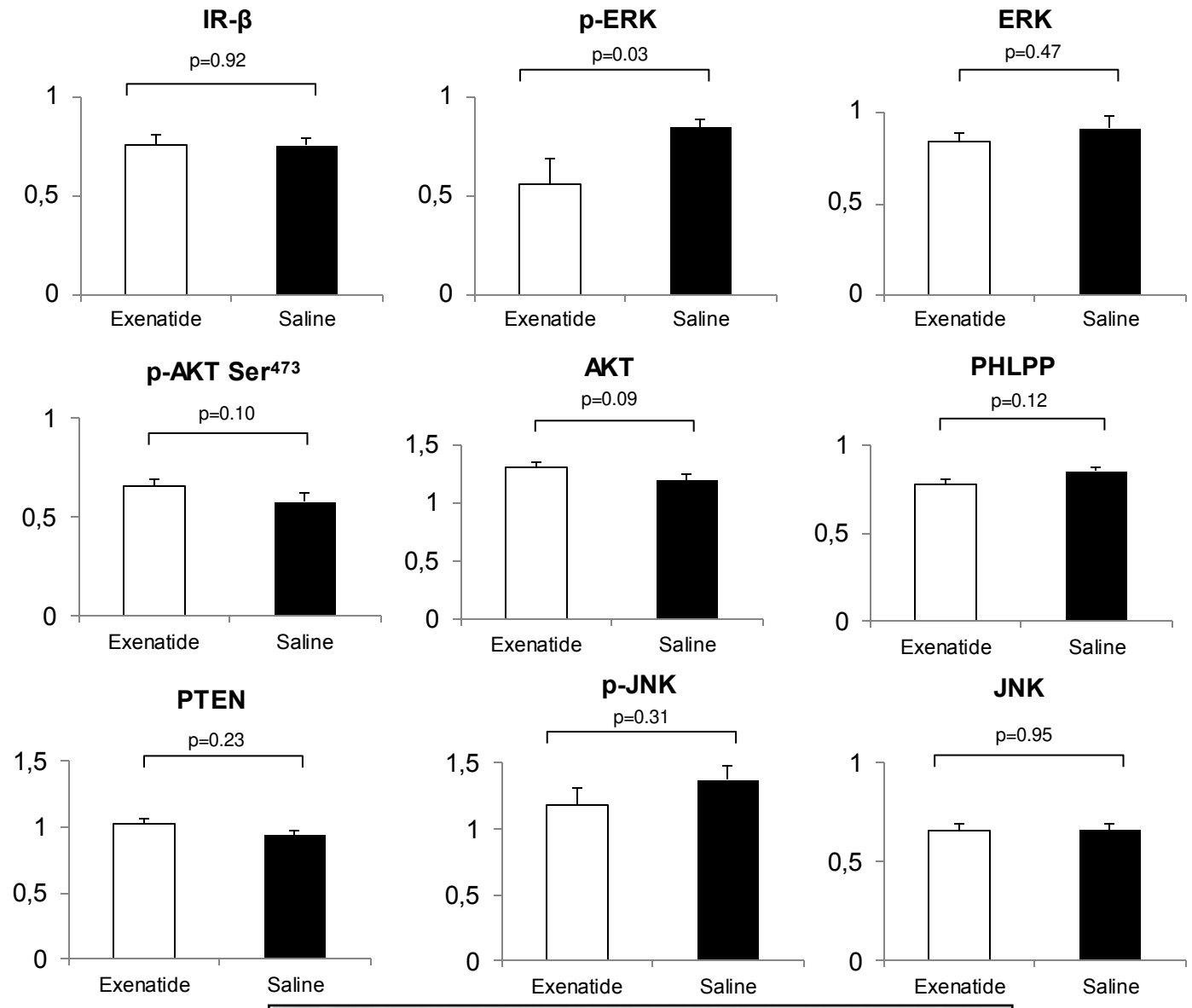

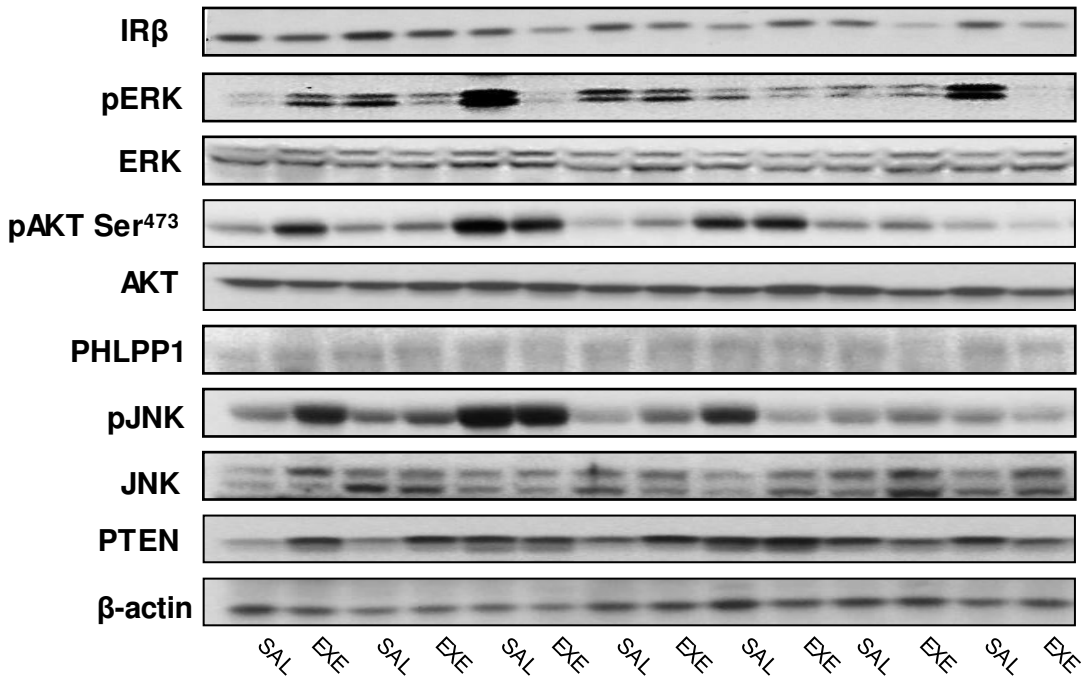

Suppl. Figure 6

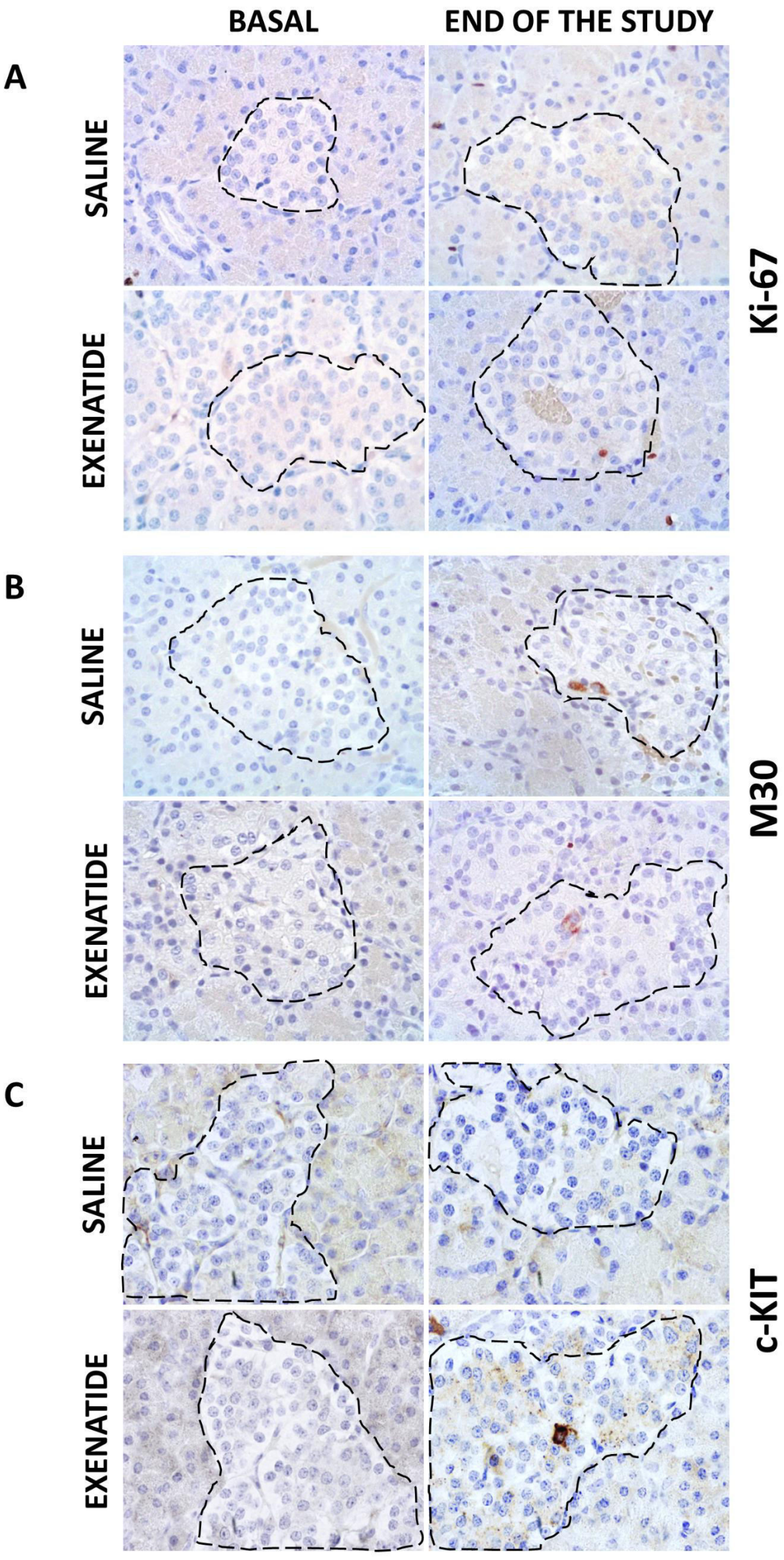

Suppl. Figure 7

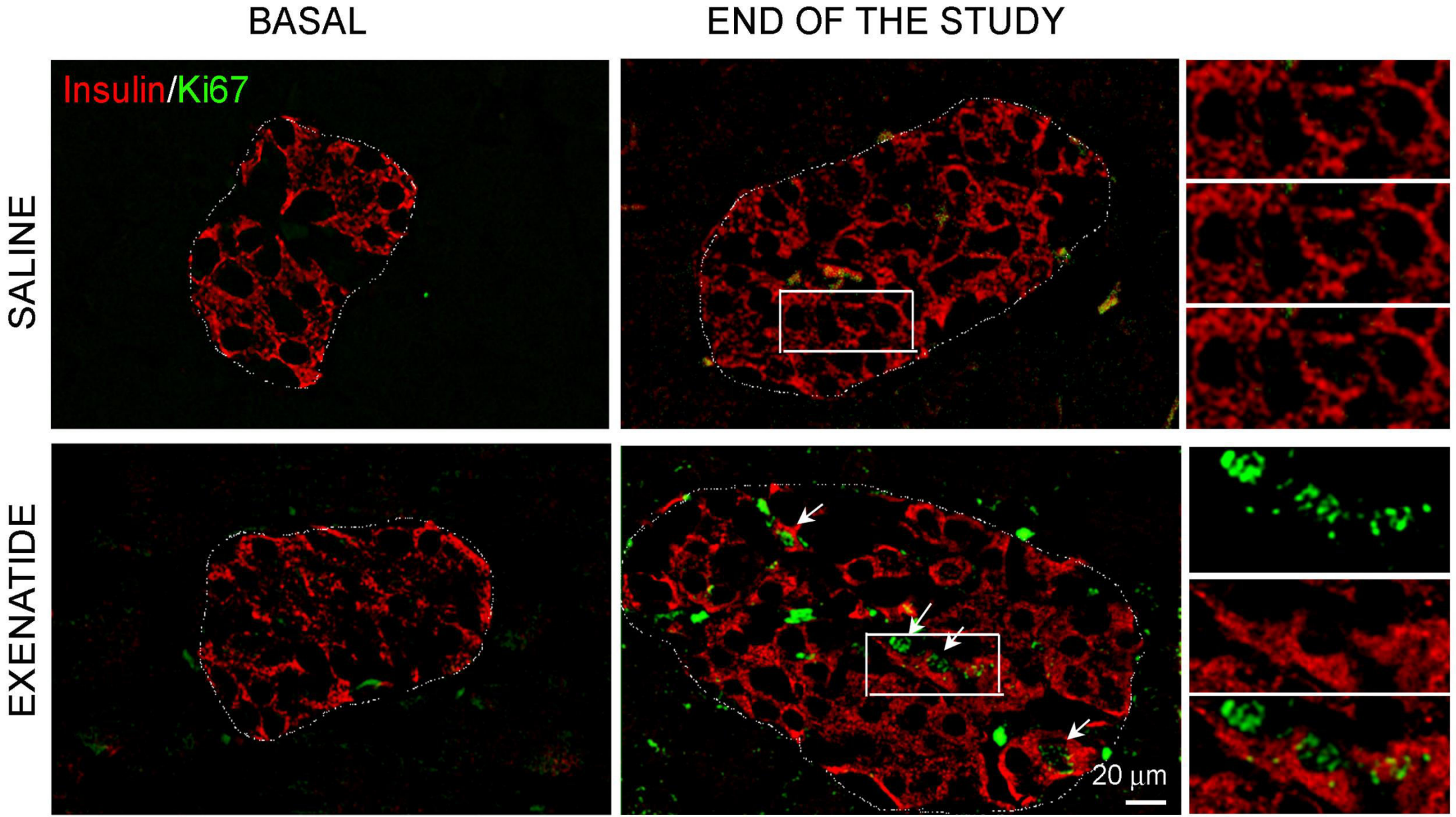

Suppl. Figure 8

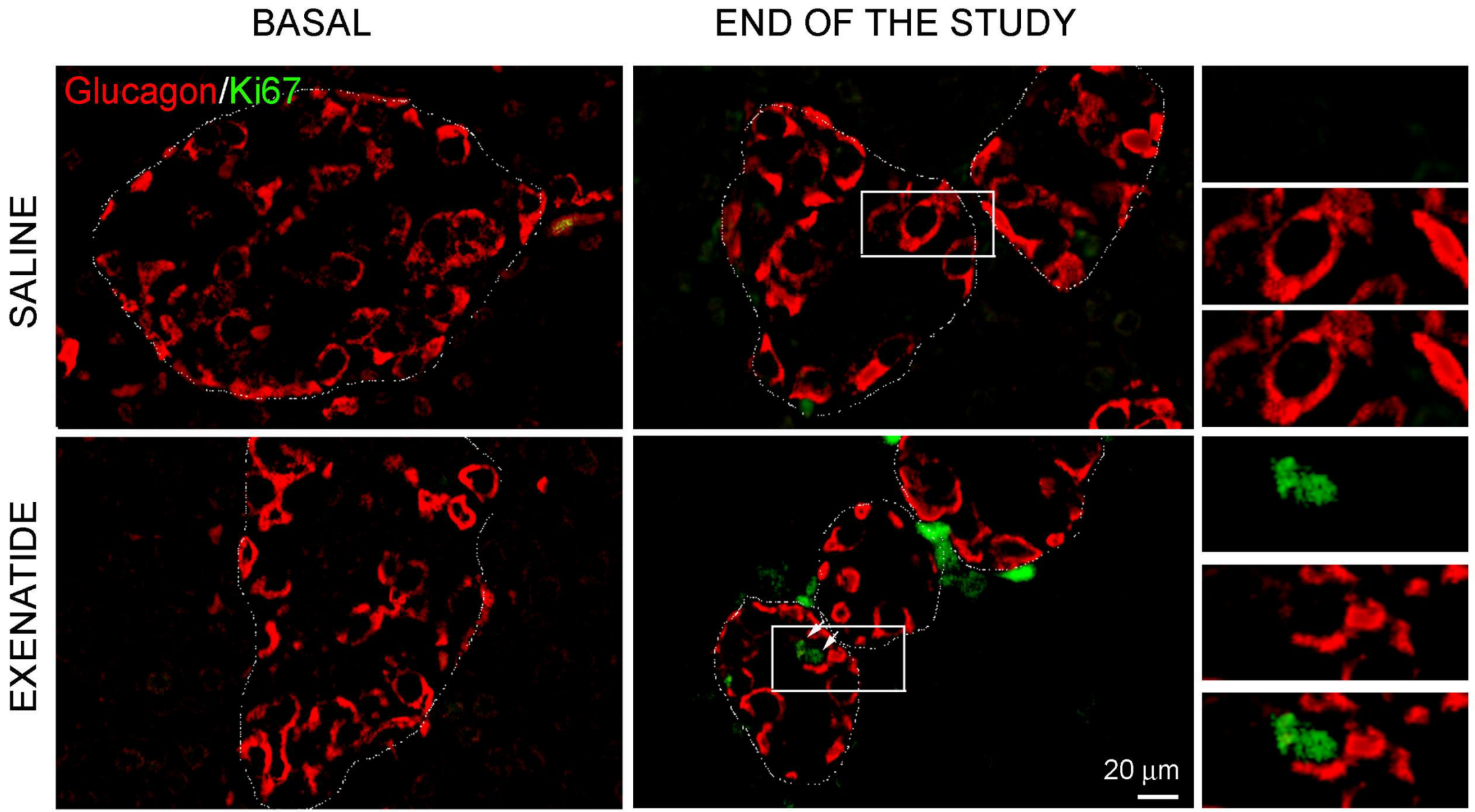

Suppl. Figure 9

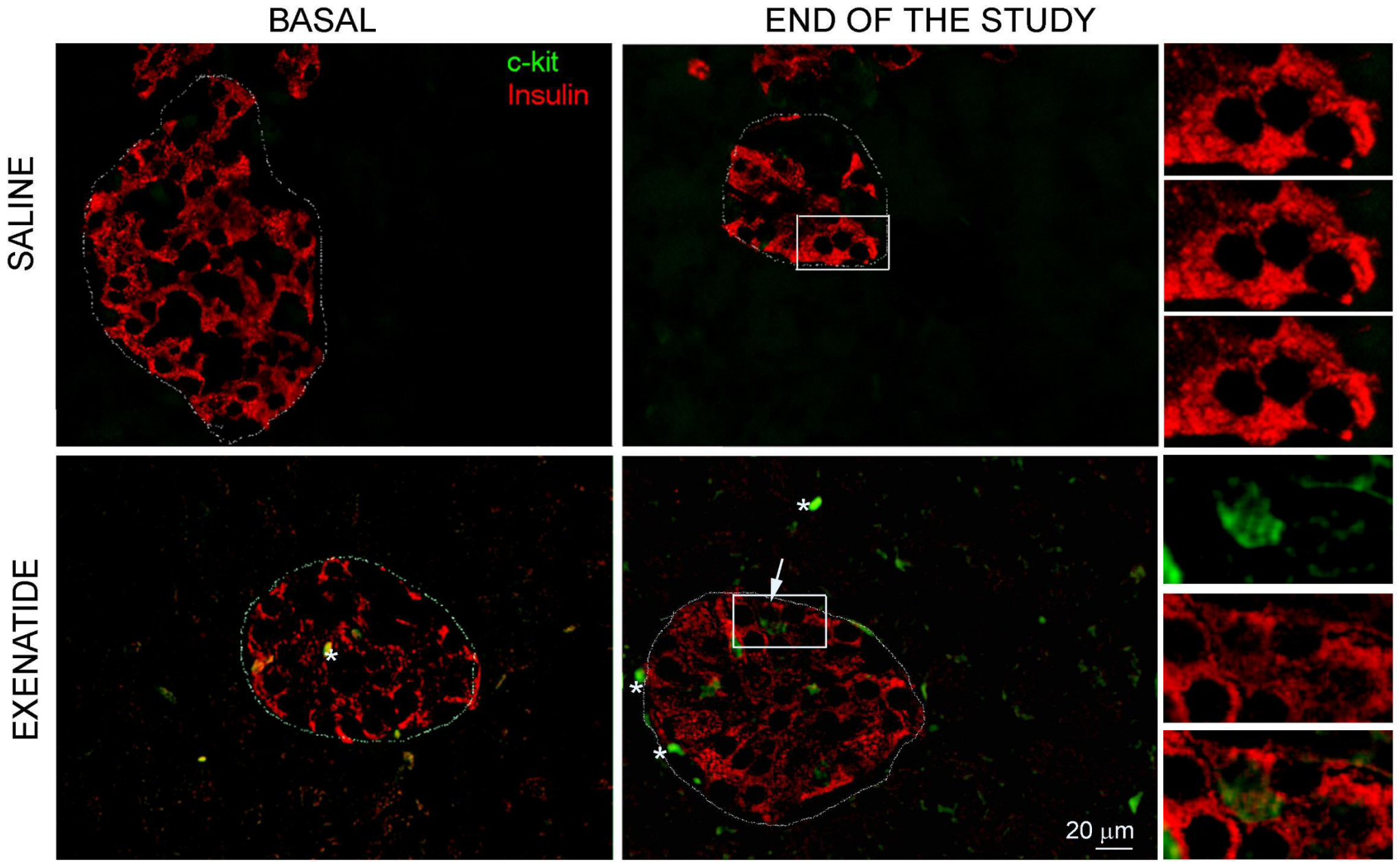

Suppl. Figure 10

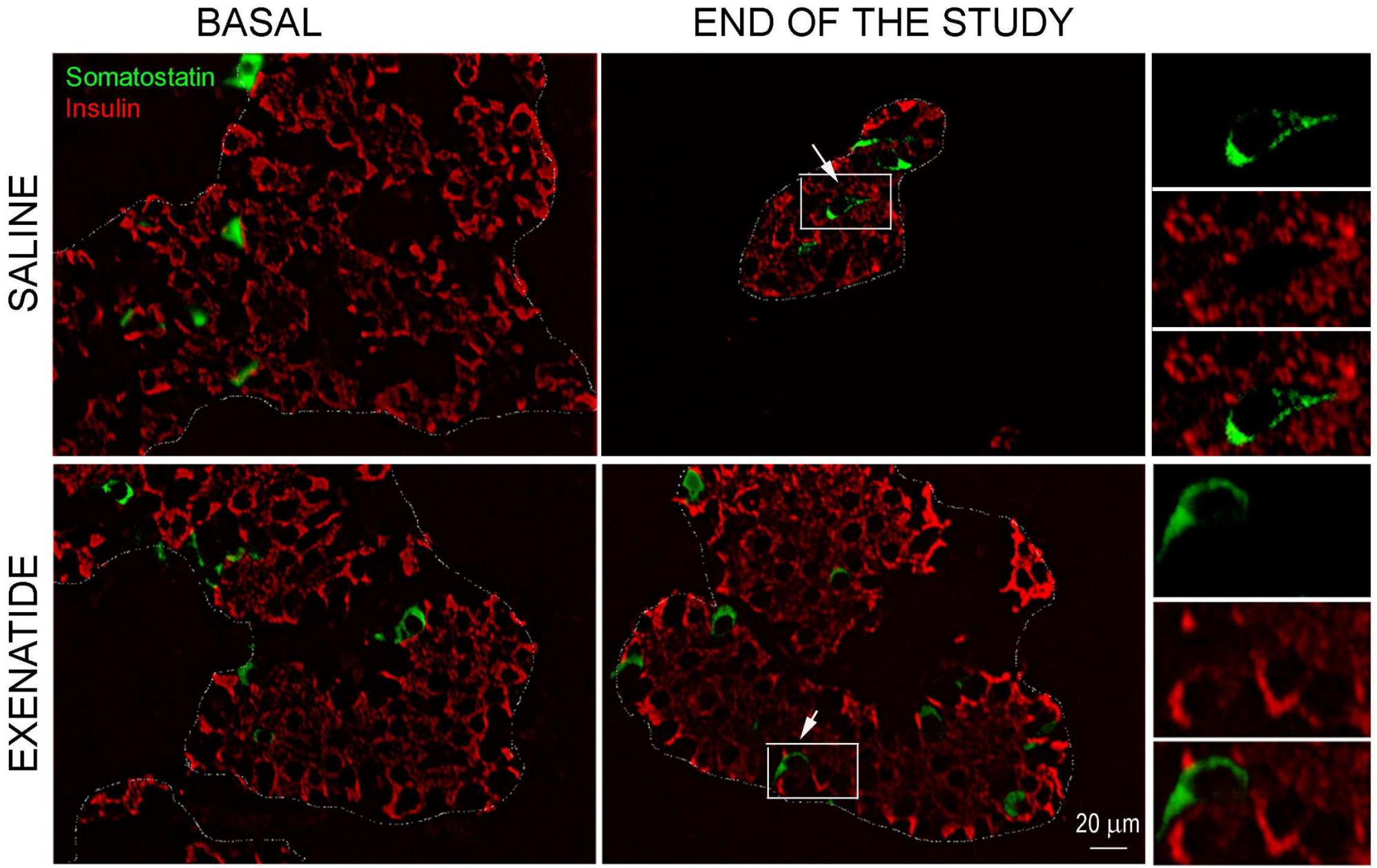

Suppl. Figure 11

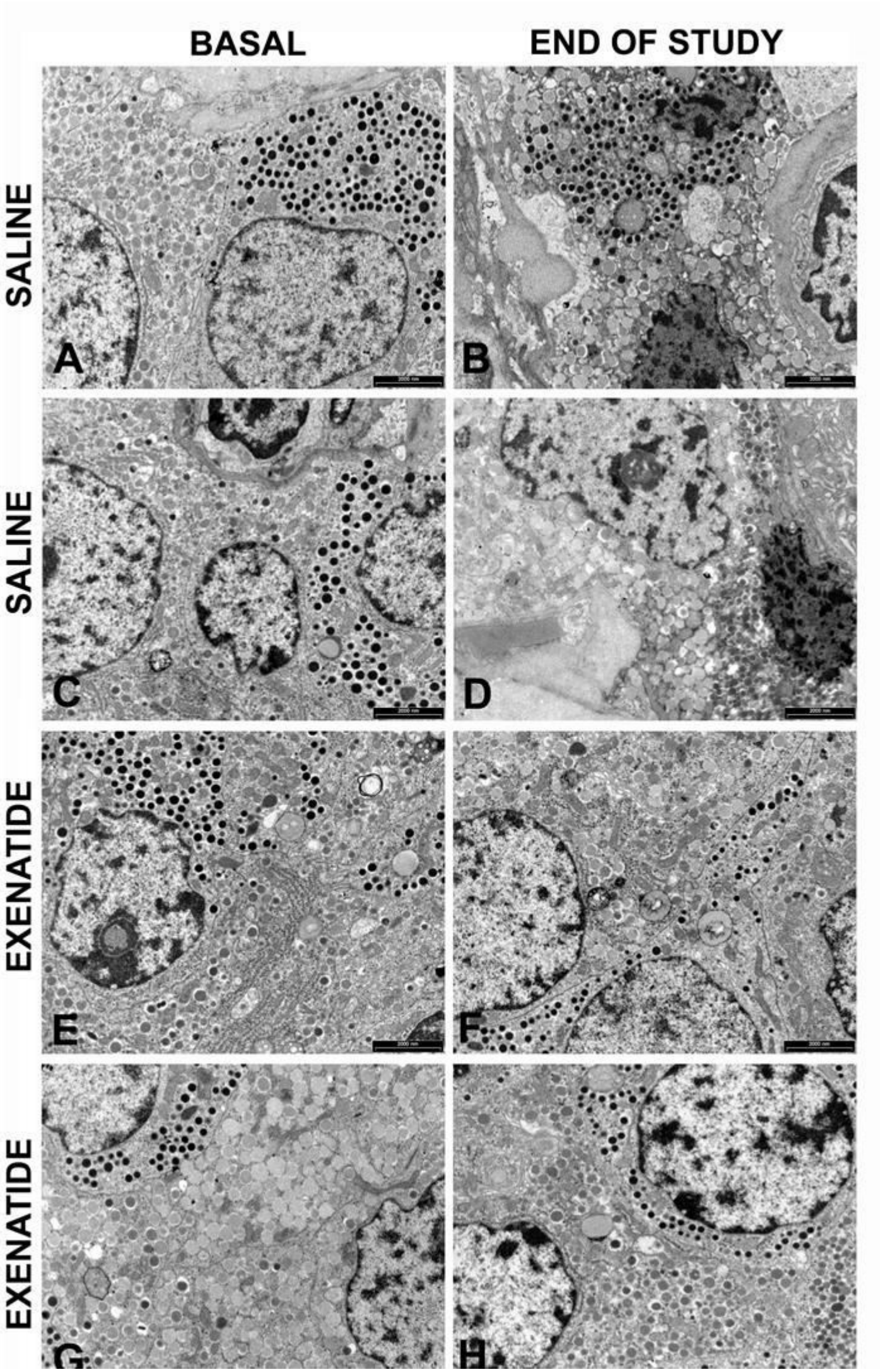

Suppl. Figure 12